with HKL[24] or XDS[25]. Crystals belong to space group $P2_12_12_1$ with unit cell dimensions $a = 56.7$ Å, $b = 67.7$ Å and $c = 135.6$ Å, and contain three molecules per asymmetric unit.

Structure determination

Selenium sites were located with SnB[26]. MAD phases were calculated with SHARP[27] and improved by density modification. A CID model was built with O[28] and refined with CNS[29]. The refined model has excellent stereochemical quality and a free *R*-factor of 25.2%. A difference Fourier for the peptide-soaked crystal was calculated with phases from the CID model and identified strong density for the CTD peptide bound to one CID molecule (chain B). The two other CID molecules pack against each other, burying their peptide-binding sites. After peptide building, the CID–CTD model was refined to a free *R*-factor of 25.7%. Peptide binding does not result in significant conformational changes in the CID domain. Soaking experiments with phosphoserine did not reveal any additional electron density.

Received 4 March; accepted 21 May 2004; doi:10.1038/nature02679.

1. Hirose, Y. & Manley, J. L. RNA polymerase II and the integration of nuclear events. *Genes Dev.* **14,** 1415–1429 (2000).
2. Proudfoot, N. J., Furger, A. & Dye, M. J. Integrating mRNA processing with transcription. *Cell* **108,** 501–512 (2002).
3. Cramer, P., Bushnell, D. A. & Kornberg, R. D. Structural basis of transcription: RNA polymerase II at 2.8Ångstrom resolution. *Science* **292,** 1863–1876 (2001).
4. Komarnitsky, P., Cho, E. J. & Buratowski, S. Different phosphorylated forms of RNA polymerase II and associated mRNA processing factors during transcription. *Genes Dev.* **14,** 2452–2460 (2000).
5. Ahn, S. H., Kim, M. & Buratowski, S. Phosphorylation of serine 2 within the RNA polymerase II C-terminal domain couples transcription and 3′ end processing. *Mol. Cell* **13,** 67–76 (2004).
6. Ni, Z., Schwartz, B. E., Werner, J., Suarez, J. R. & Lis, J. T. Coordination of transcription, RNA processing, and surveillance by P-TEFb kinase on heat shock genes. *Mol. Cell* **13,** 55–65 (2004).
7. Buratowski, S. The CTD code. *Nature Struct. Biol.* **10,** 679–680 (2003).
8. Yuryev, A. *et al.* The C-terminal domain of the largest subunit of RNA polymerase II interacts with a novel set of serine/arginine-rich proteins. *Proc. Natl Acad. Sci. USA* **93,** 6975–6980 (1996).
9. Patturajan, M., Wei, X., Berezney, R. & Corden, J. L. A nuclear matrix protein interacts with the phosphorylated C-terminal domain of RNA polymerase II. *Mol. Cell. Biol.* **18,** 2406–2415 (1998).
10. Steinmetz, E. J., Conrad, N. K., Brow, D. A. & Corden, J. L. RNA-binding protein Nrd1 directs poly(A)-independent 3′-end formation of RNA polymerase II transcripts. *Nature* **413,** 327–331 (2001).
11. Barilla, D., Lee, B. A. & Proudfoot, N. J. Cleavage/polyadenylation factor IA associates with the carboxyl-terminal domain of RNA polymerase II in *Saccharomyces cerevisiae*. *Proc. Natl Acad. Sci. USA* **98,** 445–450 (2001).
12. Misra, S., Puertollano, R., Kato, Y., Bonifacino, J. S. & Hurley, J. H. Structural basis for acidic-cluster-dileucine sorting-signal recognition by VHS domains. *Nature* **415,** 933–937 (2002).
13. Conti, E., Uy, M., Leighton, L., Blobel, G. & Kuriyan, J. Crystallographic analysis of the recognition of a nuclear localization signal by the nuclear import factor karyopherin α. *Cell* **94,** 193–204 (1998).
14. Sadowski, M., Dichtl, B., Hubner, W. & Keller, W. Independent functions of yeast Pcf11p in pre-mRNA 3′ end processing and in transcription termination. *EMBO J.* **22,** 2167–2177 (2003).
15. West, M. L. & Corden, J. L. Construction and analysis of yeast RNA polymerase II CTD deletion and substitution mutations. *Genetics* **140,** 1223–1233 (1995).
16. Suzuki, M. SPXX, a frequent sequence motif in gene regulatory proteins. *J. Mol. Biol.* **207,** 61–84 (1989).
17. Licatalosi, D. D. *et al.* Functional interaction of yeast pre-mRNA 3′ end processing factors with RNA polymerase II. *Mol. Cell* **9,** 1101–1111 (2002).
18. Verdecia, M. A., Bowman, M. E., Lu, K. P., Hunter, T. & Noel, J. P. Structural basis for phosphoserine–proline recognition by group IV WW domains. *Nature Struct. Biol.* **7,** 639–643 (2000).
19. Fabrega, C., Shen, V., Shuman, S. & Lima, C. D. Structure of an mRNA capping enzyme bound to the phosphorylated carboxy-terminal domain of RNA polymerase II. *Mol. Cell* **11,** 1549–1561 (2003).
20. Kumaki, Y., Matsushima, N., Yoshida, H., Nitta, K. & Hikichi, K. Structure of the YSPTSPS repeat containing two SPXX motifs in the CTD of RNA polymerase II: NMR studies of cyclic model peptides reveal that the SPTS turn is more stable than SPSY in water. *Biochim. Biophys. Acta.* **1548,** 81–93 (2001).
21. Cagas, P. M. & Corden, J. L. Structural studies of a synthetic peptide derived from the carboxyl-terminal domain of RNA polymerase II. *Proteins* **21,** 149–160 (1995).
22. Meredith, G. D. *et al.* The C-terminal domain revealed in the structure of RNA polymerase II. *J. Mol. Biol.* **258,** 413–419 (1996).
23. Zhang, J. & Corden, J. L. Phosphorylation causes a conformational change in the carboxyl-terminal domain of the mouse RNA polymerase II largest subunit. *J. Biol. Chem.* **266,** 2297–2302 (1991).
24. Otwinowski, Z. & Minor, W. Processing of X-ray diffraction data collected in oscillation mode. *Methods Enzymol.* **276,** 307–326 (1997).
25. Kabsch, W. Automatic processing of rotation diffraction data from crystals of initially unknown symmetry and cell constants. *J. Appl. Crystallogr.* **26,** 795–800 (1993).
26. Smith, G. D., Nagar, B., Rini, J. M., Hauptman, H. A. & Blessing, R. H. The use of SnB to determine an anomalous scattering substructure. *Acta. Crystallogr. D* **54,** 799–804 (1998).
27. Terwilliger, T. C. Automated structure solution, density modification and model building. *Acta. Crystallogr.* **58,** 1937–1940 (2002).
28. Jones, T. A., Zou, J. Y., Cowan, S. W. & Kjeldgaard, M. Improved methods for building protein models in electron density maps and the location of errors in these models. *Acta. Crystallogr. A* **47,** 110–119 (1991).
29. Brünger, A. T. *et al.* Crystallography & NMR system: A new software suite for macromolecular structure determination. *Acta. Crystallogr. D* **54,** 905–921 (1998).
30. Armache, K. J., Kettenberger, H. & Cramer, P. Architecture of initiation-competent 12-subunit RNA polymerase II. *Proc. Natl Acad. Sci. USA* **100,** 6964–6968 (2003).

Supplementary Information accompanies the paper on **www.nature.com/nature**.

Acknowledgements Part of this work was performed at the Swiss Light Source, Paul Scherrer Institut, Villigen, Switzerland. We thank C. Schulze-Briese and the staff of beamline X06SA for help; L. Jacquamet and J. McCarthy for help during data collection at the European Synchrotron Radiation Facility, Grenoble, France; G. Arnold for peptide synthesis; and K. Sträβer and members of the Cramer laboratory for careful reading of the manuscript. P.C. is supported by the Deutsche Forschungsgemeinschaft, the EMBO Young Investigator Programme and the Fonds der Chemischen Industrie. A.M. is supported by an EMBO long-term fellowship.

Competing interests statement The authors declare that they have no competing financial interests.

Correspondence and requests for materials should be addressed to P.C. (cramer@lmb.uni-muenchen.de). Atomic coordinates and structure factors for the Pcf11 CID domain and the CTD–CID complex have been deposited in the Protein Data Bank under accession numbers 1SZ9 and 1SZA, respectively.

Cyclin-dependent kinases regulate the antiproliferative function of Smads

Isao Matsuura[1,2,3], Natalia G. Denissova[1,2,3]*, Guannan Wang[1,2,3]*, Dongming He[1,2,3], Jianyin Long[1,2,3] & Fang Liu[1,2,3]

[1]*Center for Advanced Biotechnology and Medicine, and* [2]*Susan Lehman Cullman Laboratory for Cancer Research, Department of Chemical Biology, Ernest Mario School of Pharmacy, Rutgers, The State University of New Jersey, Piscataway, New Jersey 08854, USA*
[3]*Cancer Institute of New Jersey, New Brunswick, New Jersey 08903, USA*

* These authors contributed equally to this work

Transforming growth factor-β (TGF-β) potently inhibits cell cycle progression at the G1 phase[1,2]. Smad3 has a key function in mediating the TGF-β growth-inhibitory response. Here we show that Smad3 is a major physiological substrate of the G1 cyclin-dependent kinases CDK4 and CDK2. Except for the retinoblastoma protein family[3,4], Smad3 is the only CDK4 substrate demonstrated so far. We have mapped CDK4 and CDK2 phosphorylation sites to Thr 8, Thr 178 and Ser 212 in Smad3. Mutation of the CDK phosphorylation sites increases Smad3 transcriptional activity, leading to higher expression of the CDK inhibitor p15. Mutation of the CDK phosphorylation sites of Smad3 also increases its ability to downregulate the expression of c-*myc*. Using Smad3$^{-/-}$ mouse embryonic fibroblasts and other epithelial cell lines, we further show that Smad3 inhibits cell cycle progression from G1 to S phase and that mutation of the CDK phosphorylation sites in Smad3 increases this ability. Taken together, these findings indicate that CDK phosphorylation of Smad3 inhibits its transcriptional activity and antiproliferative function. Because cancer cells often contain high levels of CDK activity[5,6], diminishing Smad3 activity by CDK phosphorylation may contribute to tumorigenesis and TGF-β resistance in cancers.

Cell cycle progression from G1 to S phase is governed by CDK4 and the homologous CDK6 as well as CDK2 (ref. 4). CDK4 and CDK6 are activated by D-type cyclins at early to mid-G1 phase, whereas CDK2 is activated by E- and A-type cyclins during late G1 and S phase, respectively[4]. The activities of CDK4 and CDK6, and of CDK2, are constrained by the p16 INK4 family and the p21 Cip/Kip family inhibitors, respectively[4].

TGF-β potently inhibits cell proliferation by causing cell cycle arrest at the G1 phase[1,2]. Smad proteins can mediate TGF-β growth inhibitory responses[1,2]. In the basal state, Smad2 and Smad3 are distributed throughout cells. In response to TGF-β, Smad2 and

Smad3 are phosphorylated at the carboxyl terminus by TGF-β receptor and form complexes with Smad4 (refs 1, 2). These complexes then accumulate in the nucleus and regulate the transcription of target genes that include cell cycle regulators[1,2], such as the CDK inhibitors p15 and p21 and the protooncogene c-*myc* (refs 7–16). Smad3 is important in antiproliferative responses. For instance, hyperproliferation is a component of the carcinogenic process that leads to the development of metastatic colon cancer in Smad3$^{-/-}$ mice[17]. The loss of Smad3 expression increases susceptibility to tumorigenicity in human gastric cancer[18]. Mice lacking Smad3 display squamous hyperplasia in the stomach (C.-X. Deng, personal communication). Smad3$^{-/-}$ mice also show accelerated wound healing, partly owing to an increased rate of re-epithelialization[19]. A variety of primary cells from Smad3$^{-/-}$ mice are resistant to the growth inhibitory effects of TGF-β (refs 20–22), indicating that Smad3 has a key function in responsiveness to TGF-β.

Because Smads contain potential CDK phosphorylation sites, we analysed whether they are substrates for CDKs. To investigate whether cyclin D–CDK4 can phosphorylate Smads, we performed an *in vitro* kinase assay with endogenous CDK4 immunoprecipitated from Mv1Lu mink lung epithelial cells by an affinity-purified CDK4-specific antibody. Full-length Smad proteins fused to glutathione *S*-transferase (GST) were used as substrates. Two frequently used fusion proteins of retinoblastoma protein (Rb) with GST were included as positive controls. As shown in Fig. 1a, the highly homologous Smad2 and Smad3 were phosphorylated. Smad4, which is homologous to Smad2 and Smad3 in the amino-terminal and C-terminal domains but divergent from Smad2 and Smad3 in the middle proline-rich region, was not phosphorylated (Fig. 1a), nor was GST alone (data not shown). The phosphorylation was

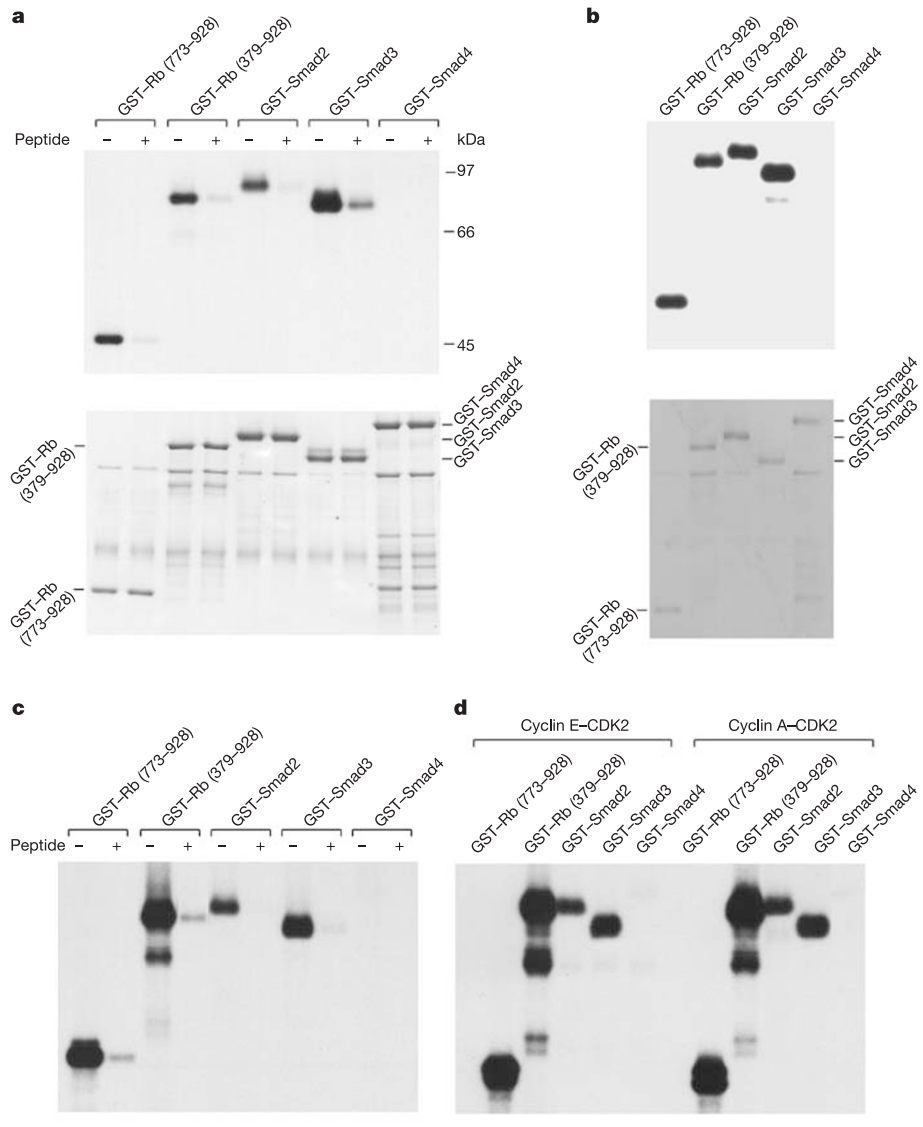

Figure 1 CDK4 and CDK2 can phosphorylate Smad3 and Smad2 *in vitro*. **a**, Top: immunoprecipitated (IP) CDK4 kinase assay. CDK4 immunoprecipitated from 240 μg Mv1Lu cell lysate with 1.2 μg CDK4 antibody in the absence or presence of 9 μg of the antigen peptide (mouse CDK4 amino acids 282–303) was used in a kinase assay with 1 μM substrates. Bottom: protein amounts indicated by Coomassie blue staining. **b**, Top: reconstituted CDK4 kinase assay. Reconstituted cyclin D–CDK4 (500 ng) was used to phosphorylate 0.4 μM substrates. Bottom: protein level indicated by Coomassie blue staining. **c**, Immunoprecipitated CDK2 kinase assay. CDK2 immunoprecipitated from 240 μg Mv1Lu cell lysate with 1.2 μg CDK2 antibody in the absence or presence of 6 μg of the antigen peptide (human CDK2 amino acids 283–298) was used in a kinase assay with 1 μM substrates. **d**, Reconstituted CDK2 kinase assay. Reconstituted cyclin E–CDK2 (13 ng) and reconstituted cyclin A–CDK2 (96 ng) were used to phosphorylate 1 μM substrates.

specific, because preincubation of the antibody with the CDK4 antigen peptide before immunoprecipitation significantly inhibited phosphorylation (Fig. 1a). Because CDK4 has a very strict substrate specificity, indicated by its inability to phosphorylate the canonical CDK substrate histone H1 (ref. 4), we further verified that CDK4 can indeed phosphorylate Smads by using bacterially expressed and *in vitro* reconstituted CDK4 (Fig. 1b). Notably, Smad3 was phosphorylated to a greater extent than Rb by immunoprecipitated CDK4 from Mv1Lu cells (Fig. 1a) and many other cell lines (data not shown) as well as by reconstituted CDK4 (Fig. 1b). Further substrate titration experiments comparing Smad3 and Rb phosphorylation by using either immunoprecipitated CDK4 or reconstituted CDK4 confirmed that Smad3 is an excellent substrate for CDK4 (Supplementary Fig. S1 and Supplementary Table S1). Similar experiments indicated that Smad3 and Smad2, but not Smad4, can also be specifically phosphorylated by immunoprecipitated CDK2 (Fig. 1c) and bacterially expressed and *in vitro* reconstituted cyclin E–CDK2 or cyclin A–CDK2 complexes (Fig. 1d).

To determine whether endogenous Smad3 is phosphorylated by G1 CDKs, we synchronized Mv1Lu cells at the G0/G1 phase by contact inhibition as described previously[23]. Cells were then released from growth arrest by plating into fresh medium and, at different time points, were labelled with ^{32}P-orthophosphate and immunoprecipitated by a Smad3-specific antibody to analyse the endogenous Smad3 phosphorylation status. Unlabelled cells prepared in parallel were analysed by flow cytometry to determine the cell cycle distribution at each time point. As shown in Fig. 2a, Smad3 phosphorylation oscillated in a cell-cycle-dependent manner. The maximal phosphorylation of Smad3 occurred at the G1/S

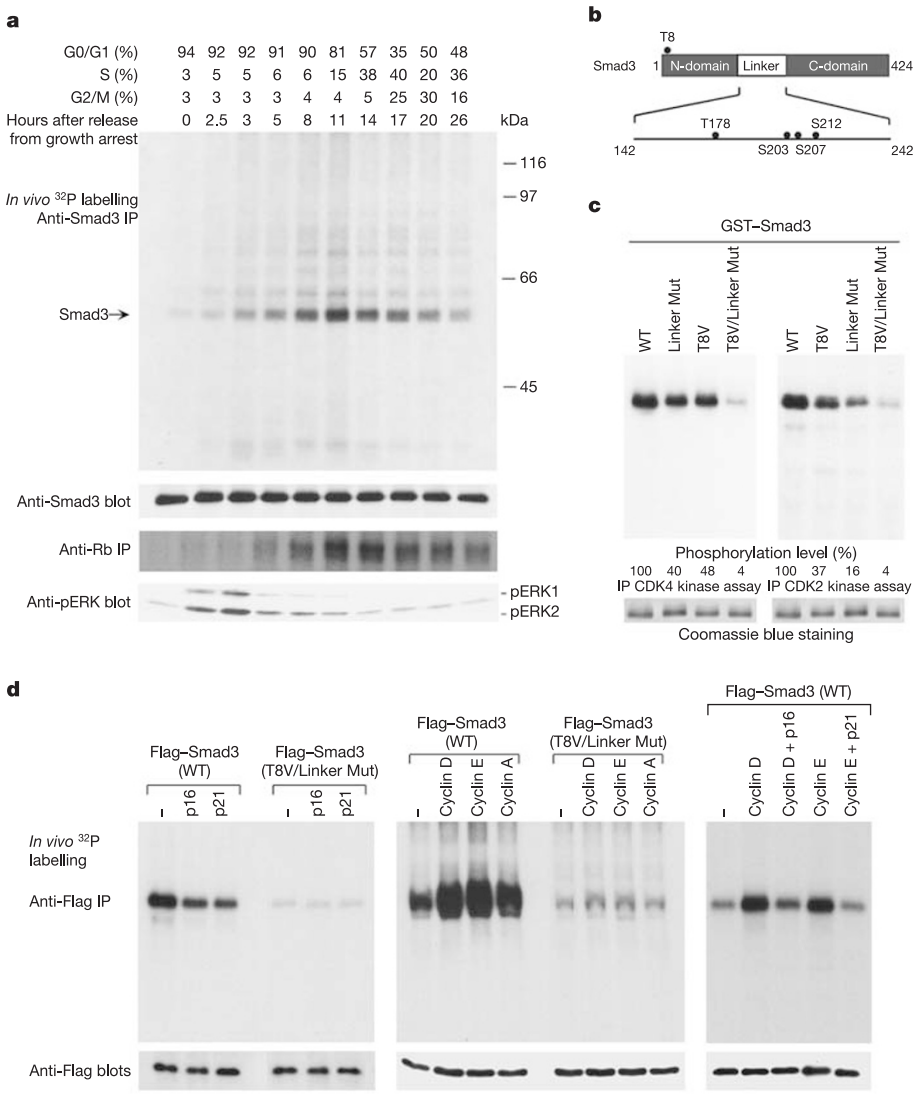

Figure 2 Smad3 is phosphorylated by endogenous G1 CDKs *in vivo*. **a**, Endogenous Smad3 is phosphorylated in a cell cycle-dependent manner. Mv1Lu cells were synchronized by contact inhibition, then plated into fresh medium, labelled with ^{32}P-orthophosphate, immunoprecipitated (IP) first with a Smad3 antibody and subsequently with an anti-Rb antibody. The ERK activity profile, analysed by a phosphotyrosine antibody that recognizes only activated ERK (pERK1 and pERK2) in unlabelled lysates, indicates that ERK might contribute to Smad3 phosphorylation at very early, but not at the peak, phosphorylation time points. **b**, Schematic diagram of Smad3 structure. **c**, Mutation of the Thr 8 and four phosphorylation sites in the Smad3 linker region markedly decreases CDK4 and CDK2 phosphorylation *in vitro*. WT, wild-type. **d**, Left, p16 or p21 transfected into Mv1Lu/L17 cells can inhibit endogenous CDK to phosphorylate Smad3. Middle and right, cyclins transfected into COS cells can activate endogenous CDKs to phosphorylate Smad3, and p16 and p21 can inhibit this activity.

junction, indicating that Smad3 was phosphorylated by G1 CDKs. Subsequent immunoprecipitation of the ^{32}P-labelled cell lysates with an antibody against Rb showed that the peak of Rb phosphorylation slightly lagged behind that of Smad3 phosphorylation (Fig. 2a), suggesting that Smad3 is a good substrate for CDK4 *in vivo*.

Smad3 contains nine potential CDK phosphorylation sites, four of which are located in the proline-rich linker region: Thr 178, Ser 203, Ser 207 and Ser 212 (Fig. 2b and Supplementary Fig. S2). The threonine at amino acid position 8 is potentially a good site, particularly for CDK4 (ref. 24). Through a number of mutational studies, we found that simultaneous mutation of Thr 8 and the four sites in the linker, designated Smad3 (T8V/Linker Mut), markedly decreased phosphorylation by CDK4 or CDK2 (Fig. 2c), indicating that CDK4 and CDK2 phosphorylation might occur within these five sites *in vitro*.

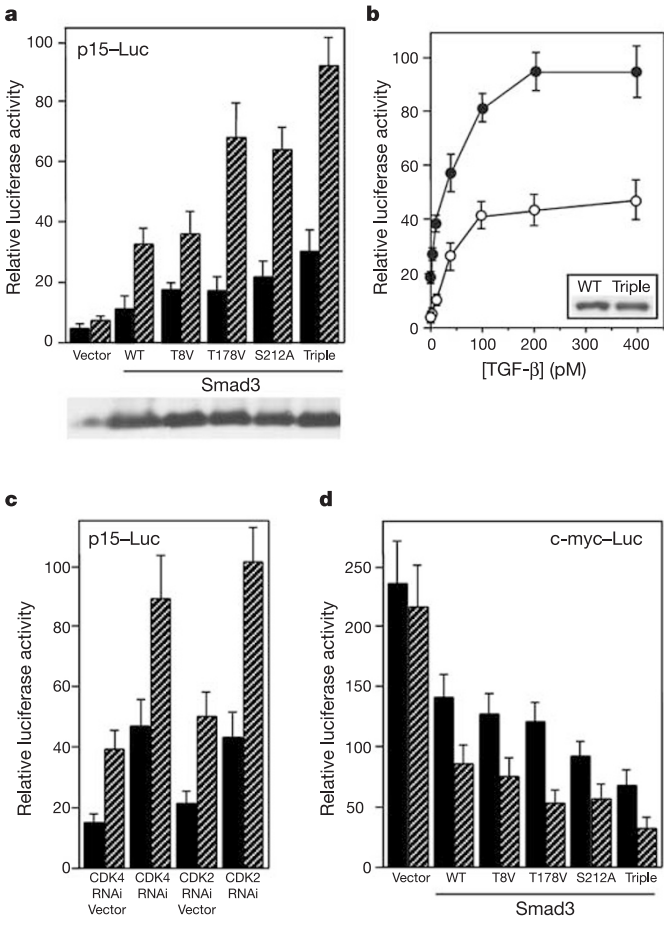

Figure 3 Mutation of CDK phosphorylation sites in Smad3 leads to an increased p15 level and reduced c-*myc* expression in reporter gene assays. **a**, Smad3$^{-/-}$ MEF were transfected with a p15 reporter gene together with the wild-type or various CDK phosphorylation mutants of Smad3. Similar results were obtained in HepG2 cells, and HepG2 cells were used to examine the Smad3 protein expression levels, as shown in the gel at the bottom. Black bars, without TGF-β; hatched bars, with TGF-β. **b**, Mv1Lu/L17 cells were transfected with a GAL4 reporter gene and TGF-β receptor along with either GAL4–Smad3 (open circles; WT) or GAL4–Smad3 (filled circles; Triple Mut), which contains the T8V, T178V and S212A mutations. **c**, CDK4 RNAi or CDK2 RNAi increases p15 reporter gene activity as analysed in HepG2 cells. Black bars, without TGF-β; hatched bars, with TGF-β. **d**, Smad3$^{-/-}$ MEF were transfected with a c-*myc* reporter gene along with the wild-type or various CDK phosphorylation mutants of Smad3 and analysed as indicated. Black bars, without TGF-β; hatched bars, with TGF-β. Error bars show standard deviation (s.d.) of at least three independent transfection results.

In transient transfection assays, Flag–Smad3 was phosphorylated, and p16 and p21 each inhibited the phosphorylation (Fig. 2d, left panel). Smad3 (T8V/Linker Mut) was phosphorylated to a much lower level than the wild-type Smad3. To determine whether the introduction of exogenous cyclins can activate endogenous CDK to phosphorylate Smad3, the wild-type or mutant version of Flag–Smad3 was cotransfected either individually or together with cyclins D, E or A. As shown in Fig. 2d (middle panel), the phosphorylation of wild-type Flag–Smad3 was significantly increased by cotransfected cyclins. The effects of cyclins D or E can be inhibited by cotransfected p16 or p21, respectively (Fig. 2d, right panel). In contrast, phosphorylation of Smad3 (T8V/Linker Mut) was only slightly increased by cyclins D or E. These observations provide additional evidence that Smad3 is phosphorylated by CDK4 and CDK2 *in vivo* and that the phosphorylation occurs within these five sites.

To determine the exact CDK phosphorylation sites in Smad3, we generated phosphopeptide antibodies against each of the five potential phosphorylation sites: Thr 8 and the four sites in the linker (Thr 178, Ser 203, Ser 207 and Ser 212). Each of the five sites was phosphorylated by both CDK4 and CDK2 *in vitro*, and only Thr 8, Thr 178 and Ser 212 were phosphorylated by CDK4 and CDK2 *in vivo* (Supplementary Figures S3–S5). To confirm that the other four potential sites (Thr 131, Ser 316, Ser 391 and Ser 415) cannot be phosphorylated by CDK, we also generated phosphopeptide antibodies against each of these sites and found that these four sites indeed cannot be phosphorylated by CDK4 or CDK2 (data not shown). Mitogen-activated protein (MAP) kinase was shown to phosphorylate Smad3 in the linker region[25]. We found that Ser 203 and Ser 207 were phosphorylated by MAP kinase and that Thr 178 was phosphorylated mostly by CDK and to a lesser extent by MAP kinase (Supplementary Fig. S5).

To analyse the role of CDK phosphorylation of Smad3, we examined the effect of mutation of the Smad3 CDK phosphorylation sites on the p15 reporter gene. As shown in Fig. 3a, each of T8V, T178V and S212A has a higher activity than the wild-type Smad3 to stimulate the p15 promoter, and the triple mutant (T8V/T178V/S212A) has the highest activity. Moreover, the GAL4–Smad3 triple mutant (T8V/T178V/S212A) has a higher activity than the wild-type GAL4–Smad3 on a GAL4–luciferase reporter gene in the absence as well as in the presence of different concentrations of TGF-β (Fig. 3b). We also found that cotransfection of CDK4 RNA-mediated interference (RNAi) or CDK2 RNAi constructs increases the basal and TGF-β-induced p15 reporter gene activity (Fig. 3c). Taken together, these results indicate that CDK phosphorylation of Smad3 can inhibit its transcriptional activity.

Smad3 also plays a critical role in the downregulation of c-*myc* expression by TGF-β (refs 13–16), which is necessary for subsequent p15 and p21 induction[1]. Mutation of Smad3 CDK phosphorylation sites also increased its ability to downregulate c-*myc* (Fig. 3d). Downregulation of c-*myc* might involve an active repression mechanism, a possibility that requires further investigation.

The above observations prompted us to ask whether Smad3 can inhibit cell cycle progression from G1 to S phase, and whether mutation of the CDK phosphorylation sites renders it more effective in executing this function. Previous studies have shown that Smad3 together with Smad2 and Smad4 activates p15 expression, and introduction of Smad3 into Smad3$^{-/-}$ mouse embryonic fibroblasts (MEF) restores the p15 reporter gene induction by TGF-β (ref. 11). Smad3$^{-/-}$ primary MEF proliferated faster than the wild-type littermate MEF in the ^{3}H-thymidine incorporation assay, and the TGF-β growth-inhibitory effects were largely lost in the Smad3$^{-/-}$ primary MEF (Fig. 4a and ref. 21). To determine whether mutation of the CDK phosphorylation sites enables Smad3 to be more effective at inhibiting G1 cell cycle progression, we generated retroviral vectors that express either the wild-type Smad3 or the

various CDK phosphorylation mutants of Smad3, and then used them to infect Smad3$^{-/-}$ primary MEF. As shown in Fig. 4b, wild-type Smad3 increased the cell population in G0/G1 phase and decreased the cell population in S phase. The various CDK phosphorylation mutants of Smad3 augmented these effects. Accordingly, these mutants were more effective than the wild-type Smad3 in inhibiting cell proliferation as measured by the ^{3}H-thymidine incorporation assay (Fig. 4c) and cell number (Fig. 4d), accompanied by increased p15 expression and lower c-Myc levels (Fig. 4e). In addition to the Smad3$^{-/-}$ primary MEF, we have also

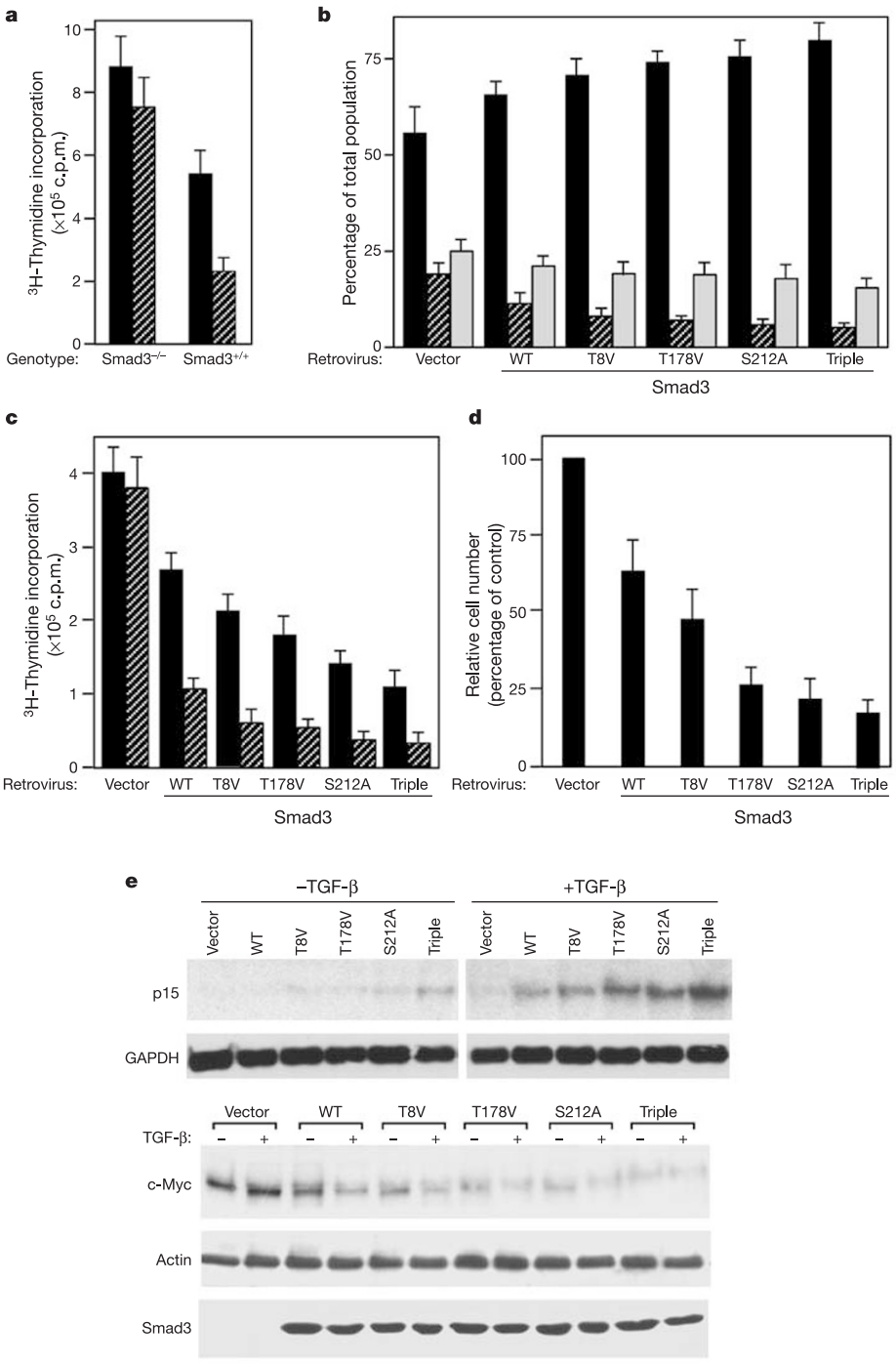

Figure 4 Mutation of the CDK phosphorylation sites in Smad3 leads to increased antiproliferative activities. **a**, Smad3$^{-/-}$ primary MEF and the wild-type littermate control MEF (both at passage 3) were compared in a ^{3}H-thymidine incorporation assay in the absence (black bars) and in the presence (hatched bars) of TGF-β. The average of four experiments is shown. Error bars represent standard deviation (s.d.). **b**–**e**, Smad3$^{-/-}$ primary MEF (passage 3) were infected with retrovirus vector, retroviral wild-type Smad3 or various Smad3 CDK phosphorylation mutants. Infected cells were then split and seeded for fluorescence-activated cell sorting analysis 2 days later (**b**; black bars, G0/G1 phase; hatched bars, S phase; grey bars, G2/M phase), ^{3}H-thymidine incorporation assay (**c**; black bars, without TGF-β; hatched bars, with TGF-β), measurement of cell number about 5 days later (**d**) and analysis of p15 and c-Myc levels (**e**). The error bars in **b**–**d** represent s.d. of four experiments. The infected MEF were treated with TGF-β for 24 h in **e**. Total RNA (10 μg) and protein (15 μg) were analysed by northern blot (top) and immunoblotting (bottom), respectively.

observed the same trend in other cell types including the Mv1Lu epithelial cells, which contain relatively low levels of wild-type Smad3 (data not shown). Taken together, these observations indicate that phosphorylation of Smad3 by CDK facilitates cell cycle progression from G1 to S phase.

Thus, we have shown that Smad3 is phosphorylated by CDK4 and CDK2. Mutation of its CDK phosphorylation sites increases its transcriptional activity and antiproliferative function. We propose that under physiological conditions, phosphorylation of Smad3 by CDK inhibits its transcriptional activity, contributing to a decreased level of p15 and an increased level of c-Myc, thus facilitating cell cycle progression from G1 to S phase. In the presence of physiological concentrations of TGF-β, normal cells are inhibited by TGF-β. However, cancer cells often contain high levels of CDK activities because of frequent amplification, translocation or overexpression of the cyclin D1 gene or inactivation of the tumour suppressor p16 (refs 5, 6). In addition, overexpression of cyclin E and decreases in CDK inhibitor p27 levels also occur in cancer cells[26]. Inactivation of Smad3 and presumably the homologous Smad2 by extensive CDK phosphorylation may provide an important mechanism for resistance to the TGF-β growth-inhibitory effects in cancers. □

Methods

Phosphorylation *in vitro* by immunoprecipitated CDK

Mv1Lu cells were lysed in a buffer containing 50 mM Tris pH 7.5, 150 mM NaCl, 0.5% Nonidet P40, 1 mM dithiothreitol (DTT) and protease and phosphatase inhibitors. Antibodies against CDK2 (M2) and CDK4 (C-22) from Santa Cruz Biotechnology were used for immunoprecipitations. The kinase reaction was carried out for 1 h in 30 μl containing 50 mM HEPES pH 7.4, 15 mM $MgCl_2$, 1 mM EGTA, 0.1% Tween 20, 1 mM DTT, 50 μM ATP, 5 μCi [γ-^{32}P]ATP (3000 Ci mmol^{-1}) and substrates at 30 °C. GST–Rb (773–928) contains the proline-rich region, and GST–Rb (379–928) contains in addition the Rb pocket domain.

Phosphorylation *in vitro* by reconstituted CDK

GST–CDK4, GST–CDK2 and His-tagged cyclins D, E and A were expressed and purified from *Escherichia coli* as described previously[27]. GST–CDK and His–cyclin were mixed and incubated with HeLa extracts in the presence of ATP and Mg^{2+} to activate CDK4 or CDK2. Cyclin D–CDK4 was reconstituted as described previously[28] except that no $MnCl_2$ was included. The cyclin D–CDK4 complex was then purified with glutathione agarose beads. Cyclin E–CDK2 and cyclin A–CDK2 were reconstituted as described previously[27] and purified by successive Ni-nitrilotriacetate–agarose and glutathione–agarose chromatography. The purified cyclin–CDK complexes were used to phosphorylate substrates for 40 min in 20 μl reactions containing 35 mM HEPES pH 7.4, 10 mM $MgCl_2$, 1 mM EGTA, 0.1% Tween 20, 1 mM DTT, 15 μM ATP and 5 μCi [γ-^{32}P]ATP for CDK4 or 100 μM ATP and 2 μCi [γ-^{32}P]ATP for CDK2 at 30 °C.

Phosphorylation *in vivo*

For analysis of endogenous Smad3 phosphorylation, Mv1Lu mink lung epithelial cells were synchronized at G0/G1 phase by contact inhibition in complete medium as previously described[23]. In brief, Mv1Lu cells were grown to full confluence in complete medium. Cells were then split and plated into fresh medium. At different time points, cells were phosphate-starved for 0.5 h and then labelled for 1.5 h with 1 mCi ml^{-1} ^{32}P-orthophosphate. Cells were lysed in a buffer containing 10 mM Tris pH 7.8, 150 mM NaCl, 1 mM EDTA, 1% Nonidet P40, and protease and phosphatase inhibitors, and immunoprecipitated by a Smad3-specific antibody. For analysis of transfected Flag-tagged Smad3 phosphorylation, Mv1Lu/L17 or COS cells were transfected by DEAE-dextran. At 30–36 h after transfection, cells were phosphate-starved for 45 min and labelled with ^{32}P-orthophosphate at 1 mCi ml^{-1} for 2.5 h followed by immunoprecipitation by a Flag antibody.

Retrovirus production

Wild-type or CDK phosphorylation mutant Smad3 were subcloned into the retroviral vector pLZRSΔ-IRES–GFP[29] and transfected into ecotropic phoenix packaging cells to produce retroviruses as described previously[30]. Smad3$^{-/-}$ MEF were infected at greater than 90% efficiency.

Generation of MEF and ^{3}H-thymidine incorporation assay

Smad3$^{+/-}$ mice were crossed and MEF were generated as described previously[21]; 2×10^5 Smad3$^{-/-}$ primary MEF and the wild-type littermate control MEF (both at passage 3) were seeded in six-well plates for 24 h, then treated for 24 h with or without 500 pM TGF-β. During the last 4 h, 5 μCi of ^{3}H-thymidine was added to the culture, and ^{3}H-thymidine incorporation was assayed as described previously[21].

Received 5 January; accepted 10 May 2004; doi:10.1038/nature02650.

1. Massagué, J., Blain, S. W. & Lo, R. S. TGF-β signaling in growth control, cancer, and heritable disorders. *Cell* **103,** 295–309 (2000).
2. Derynck, R., Akhurst, R. J. & Balmain, A. TGF-β signaling in tumor suppression and cancer progression. *Nature Genet.* **29,** 117–129 (2001).
3. Weinberg, R. A. The retinoblastoma protein and cell cycle control. *Cell* **81,** 323–330 (1995).
4. Sherr, C. J. & Roberts, J. M. CDK inhibitors: positive and negative regulators of G1-phase progression. *Genes Dev.* **13,** 1501–1512 (1999).
5. Hall, M. & Peters, G. Genetic alterations of cyclins, cyclin-dependent kinases, and Cdk inhibitors in human cancer. *Adv. Cancer Res.* **68,** 67–108 (1996).
6. Sherr, C. J. Cancer cell cycles. *Science* **274,** 1672–1677 (1996).
7. Hannon, G. J. & Beach, D. p15^{INK4B} is a potential effector of TGF-β-induced cell cycle arrest. *Nature* **371,** 257–261 (1994).
8. Li, J. M., Nichols, M. A., Chandrasekharan, S., Xiong, Y. & Wang, X.-F. Transforming growth factor β activates the promoter of cyclin-dependent kinase inhibitor p15^{INK4B} through an Sp1 consensus site. *J. Biol. Chem.* **270,** 26750–26753 (1995).
9. Moustakas, A. & Kardassis, D. Regulation of the human p21/WAF1/Cip1 promoter in hepatic cells by functional interaction between Sp1 and Smad family members. *Proc. Natl Acad. Sci. USA* **95,** 6733–6738 (1998).
10. Pardali, K. *et al.* Role of Smad proteins and transcription factor Sp1 in p21$^{Waf1/Cip1}$ regulation by transforming growth factor-β. *J. Biol. Chem.* **275,** 29244–29256 (2000).
11. Feng, X.-H., Lin, X. & Derynck, R. Smad2, Smad3 and Smad4 cooperate with Sp1 to induce p15^{Ink4B} transcription in response to TGF-β. *EMBO J.* **19,** 5178–5193 (2000).
12. Seoane, J., Le, H. V., Shen, L., Anderson, S. A. & Massague, J. Integration of Smad and forkhead pathways in the control of neuroepithelial and glioblastoma cell proliferation. *Cell* **117,** 211–223 (2004).
13. Chen, C. R., Kang, Y. & Massagué, J. Defective repression of c-*myc* in breast cancer cells: A loss at the core of the transforming growth factor growth arrest program. *Proc. Natl Acad. Sci. USA* **98,** 992–999 (2001).
14. Yagi, K. *et al.* c-myc is a downstream target of the Smad pathway. *J. Biol. Chem.* **277,** 854–861 (2002).
15. Chen, C.-R., Kang, Y., Siegel, P. M. & Massagué, J. E2F4/5 and p107 as Smad cofactors linking the TGF-β receptor to c-*myc* repression. *Cell* **110,** 19–32 (2002).
16. Frederick, J. P., Liberati, N. T., Waddell, D. S., Shi, Y. & Wang, X. F. Transforming growth factor beta-mediated transcriptional repression of c-myc is dependent on direct binding of Smad3 to a novel repressive Smad binding element. *Mol. Cell. Biol.* **24,** 2546–2559 (2004).
17. Zhu, Y., Richardson, J. A., Parada, L. F. & Graff, J. M. Smad3 mutant mice develop metastatic colorectal cancer. *Cell* **94,** 703–714 (1998).
18. Han, S. U. *et al.* Loss of the Smad3 expression increases susceptibility to tumorigenicity in human gastric cancer. *Oncogene* **23,** 1333–1341 (2004).
19. Ashcroft, G. S. *et al.* Mice lacking Smad3 show accelerated wound healing and an impaired local inflammatory response. *Nature Cell Biol.* **1,** 260–266 (1999).
20. Yang, X. *et al.* Targeted disruption of SMAD3 results in impaired mucosal immunity and diminished T cell responsiveness to TGF-β. *EMBO J.* **18,** 1280–1291 (1999).
21. Datto, M. B. *et al.* Targeted disruption of Smad3 reveals an essential role in transforming growth factor β-mediated signal transduction. *Mol. Cell. Biol.* **19,** 2495–2504 (1999).
22. Rich, J. N., Zhang, M., Datto, M. B., Bigner, D. D. & Wang, X.-F. Transforming growth factor-β-mediated p15^{INK4B} induction and growth inhibition in astrocytes is Smad3-dependent and a pathway prominently altered in human glioma cell lines. *J. Biol. Chem.* **274,** 35053–35058 (1999).
23. Laiho, M., DeCaprio, J. A., Ludlow, J. W., Livingston, D. M. & Massagué, J. Growth inhibition by TGF-β linked to suppression of retinoblastoma protein phosphorylation. *Cell* **62,** 175–185 (1990).
24. Kitagawa, M. *et al.* The consensus motif for phosphorylation by cyclin D1-Cdk4 is different from that for phosphorylation by cyclin A/E-Cdk2. *EMBO J.* **15,** 7060–7069 (1996).
25. Kretzschmar, M., Doody, J., Timokhina, I. & Massagué, J. A mechanism of repression of TGF-β/Smad signaling by oncogenic ras. *Genes Dev.* **13,** 804–816 (1999).
26. Porter, P. L. *et al.* Expression of cell-cycle regulators p27Kip1 and cyclin E, alone and in combination, correlate with survival in young breast cancer patients. *Nature Med.* **3,** 222–225 (1997).
27. Matsuura, I. & Wang, J. Demonstration of cyclin-dependent kinase inhibitory serine/threonine kinase in bovine thymus. *J. Biol. Chem.* **271,** 5443–5450 (1996).
28. Phelps, D. E. & Xiong, Y. Assay for activity of mammalian cyclin D-dependent kinases CDK4 and CDK6. *Methods Enzymol.* **283,** 194–204 (1997).
29. Kim, M. J. *et al. Nkx3.1* mutant mice recapitulate early stages of prostate carcinogenesis. *Cancer Res.* **62,** 2999–3004 (2002).
30. Swift, S., Lorens, J., Achacoso, P. & Nolan, G. P. Rapid production of retroviruses for efficient gene delivery to mammalian cells using 293T cell-based systems. in *Curr. Protocols Immunol.* (eds Coligan, J. E. *et al.*) Unit 10.28, Suppl. 31 (John Wiley & Sons, 1999).

Supplementary Information accompanies the paper on **www.nature.com/nature**.

Acknowledgements We are very grateful to X.-F. Wang for Smad3 mutant mice; E. P. Reddy, R. V. Mettus and H. Kiyokawa for CDK4 mutant mice; J. Massagué for reagents and continued support; C.-X. Deng for reagents and communications before publication; M. M. Shen and members of his laboratory for assistance with mouse work; C. Abate-Shen, M. Cobb, X.-F. Feng, J. Germino, G. J. Hannon, S.-J. Kim, M. Kretzschmar, H. Lee, M.-H. Lee, E. Lees, X. Liu, H. L. Moses, G. Nolan, A. Rabson, D. Reinberg, M. Reiss, Y. Shi, N. Walworth and W. Xie for reagents and/or suggestions; and numerous colleagues for discussions. This work was supported by the 1999 American Association for Cancer Research–National Foundation for Cancer Research Career Development Award, a Burroughs Wellcome Fund New Investigator Award, a Kimmel Scholar Award from the Sidney Kimmel Foundation for Cancer Research, the Emerald Foundation, the New Jersey Commission on Cancer Research, and the NIH (to F.L.).

Competing interests statement The authors declare that they have no competing financial interests.

Correspondence and requests for materials should be addressed to F.L. (fangliu@cabm.rutgers.edu).